DOI: 10.5604/20830157.1148043

FUZZY EVALUATION OF VISUAL CONNECTEDNESS IN THERMOGRAPHY IMAGES OF CYLINDRICAL SURFACE

Tomasz Jaworski, Jacek Kucharski
Lodz University of Technology, Institute of Applied Computer Science

Abstract. *This article presents an idea of visual connectedness measure between components in thermography images of rotating steel roller, cylindrically shaped. Both definition and method of measure calculus is given along with a short discussion.*

Keywords: fuzzy logic, thermovision, thermal image decomposition, visual connectedness

ROZMYTA OCENA SPÓJNOŚCI WIZUALNEJ W OBRAZACH TERMOWIZYJNYCH POWIERZCHNI WALCOWEJ

Streszczenie. *Artykuł przedstawia metodę oceny spójności wizualnej komponentów temperaturowych w obrazach termowizyjnych obracającego się walca. Zaproponowano definicję oraz metodę wyznaczania wartości oceny spójności.*

Słowa kluczowe: logika rozmyta, termowizja, dekompozycja termografu, spójność wizualna

Introduction

Computational intelligence, able to imitate human perception along with decision making, expansively applies to many research fields. From the most basic, such as industry/production through data analysis and monitoring, to defense systems, simulating human expert with a computer software gains advantages, such as repeatability, fatigue-freedom or low-cost operation.

One of the most important fields mentioned is image description and understanding. Classical image is a set of pixels, RGB or monochromatic, amount of which highly extends 10^6. Any inference or data analysis on such amount of information is hard to investigate or simply time consuming (critical in real-time systems).

In this paper the authors propose a method that, for a given type of thermal image, generates a description on level of abstraction higher than pixels, based on so called *visual connectedness*. The obtained results can be used to develop advanced inferring methods of such images or to improve the existing ones, e.g. temperature regulators. The presented method is designed to analyze temperature distribution images of rotating steel cylinder's surface intended for paper milling industry.

The important feature of the problem under consideration is that the thermal processes that take place on the surface of the heated object result in thermographs that are particularly fuzzy and irregular. Those images can be relatively easily analyzed by humans, however they are not very manageable to the typical procedures of automated image processing. Moreover, the non-contact temperature field imaging of a rotating cylindrical roller, requires the use of specific methods at the data acquisition stage. It is also important to mention that additional sources of expertise in the discussed problem are: 1) a partial knowledge of the physical cause-effect relations that are observed in the obtained thermal images; 2) a qualitative description of the observation method for such images given by an experienced operator – a process expert. However, both the knowledge about physical phenomena and the description of human expert behavior are incomplete and imprecise. Hence a formal tool of choice, naturally suited to use in this type of task, is the fuzzy sets and fuzzy logic theory.

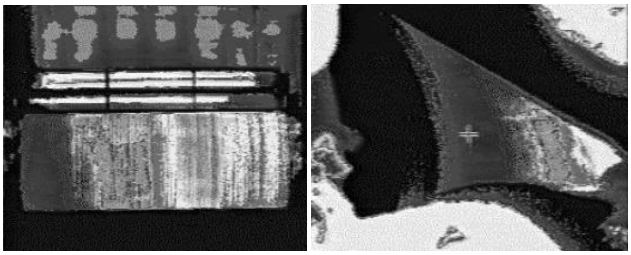

Fig. 1. A temperature distribution on a paper sheet as a consequence of moisture inhomogeneity [8]

We believe that proposed evaluation method will be useful in moisture distribution control problems [8], as they are closely related with paper sheet's temperature (see Fig. 1).

1. Description of a thermal image

Every thermal image of a plain surface can be considered as a sum (superposition) of responses to heat pulses, generated over the surface [9, 23]. Heating source depends on technological process and expected outcome. Most common are laser point [15] and inductive heating [5, 6, 13]. Due to physical heat flux distribution of a given source (often denoted as $\partial Q/dS$), the set of pulses is not directly given. To bypass this inconvenience, the authors propose a definition of a *temperature component* along with a method to represent an input image in terms of those components.

Moreover, recognizing the thermal image representation as a thermal pulse responses superposition of inductively heated surface with further clustering of such type of basic temperature components (information granules) based on proposed visual connectedness fuzzy evaluation, allows to identify coherent areas of the heated object that have certain thermal state. This leads to a image processing method that is sensitive to the physical phenomena responsible for shape of observed images.

1.1. Definition of a temperature component

A *temperature component* describes a temperature distribution on a plain surface and can be considered as a pulse response to a point heat source. Such component can be denoted as an ordered four (1), with its representation in spatial-temperature domain given by (2).

$$K_n = \left(\Theta_n, r_n, x_n, y_n\right) \tag{1}$$

where: Θ [°C] – peak temperature of the n-th component (its height) but with omitted ambient temperature; r [m] – radius of the component; x, y [m] – its localization on the surface.

$$\Gamma_n\left(\mathbf{p}\right) = \Theta_n \exp\left(-\frac{\left\|\mathbf{p}-\left|x_n;\mathrm{y}_n\right|\right\|^2}{r_n}\right) + \tag{2}$$

$$+\Theta_n \exp\left(-\frac{1}{r_n}\left\|\mathbf{p}-\begin{vmatrix} x_n+2\pi C_R;\mathrm{y}_n \end{vmatrix} \quad \text{for } p_y < \pi C_R\right\|^2\right)$$

$$\left\|\mathbf{p}-\begin{vmatrix} x_n-2\pi C_R;\mathrm{y}_n \end{vmatrix} \quad \text{for } p_y \geq \pi C_R\right\|$$

where: $\Gamma_n(\mathbf{p})$[°C] – temperature of n-th component in point $\mathbf{p}\in\Re^2$; C_R [m] – radius of the cylinder.

The reason behind the bell-shape of (2) is the nature of heat transfer problems; it results from the solution of differential heat conduction equation for point source heat pulse [4, 9, 12, 31]. The sum of two *exp* functions allows to take the observed object's cylindrical geometry into account.

Input image can be approximately represented by a finite set of components (1), denoted as **K** (3).

$$\mathbf{K} = \{K_n : n = 1..N\} \tag{3}$$

where: N – number of components in set **K**

Having a set **K**, one can calculate an approximation of input image in terms of components K. It can be defined as an image with characteristic function given by (4).

$$i(\mathbf{p}) = \sum_{n=1..|\mathbf{K}|} \Gamma_n(\mathbf{p}) \tag{4}$$

where: |**K**| - number of components in set **K**, **p** – pixel coordinates on image surface

1.2. Image source

Test images were obtained with use of a model developed by the authors [13], see Fig. 2. It is a coated steel cylinder of length 1,2m and 20cm radius, driven by a motor-inverter module.

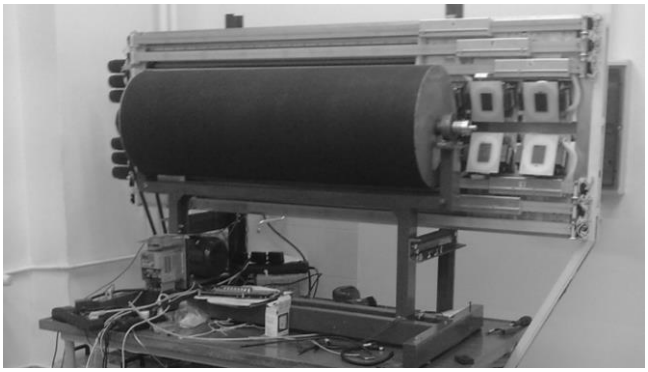

Fig. 2. The physical model of a roller

The heat source is provided by a set of 6 movable inductive heaters [7], with 1kW of power dispatch per each. Heaters are driven horizontally and can be placed or moved anywhere along the horizontal axis. Images are acquired by a Flir A615 infrared camera synchronized with cylinder's angular position by a quadrature incremental encoder, connected to its shaft.

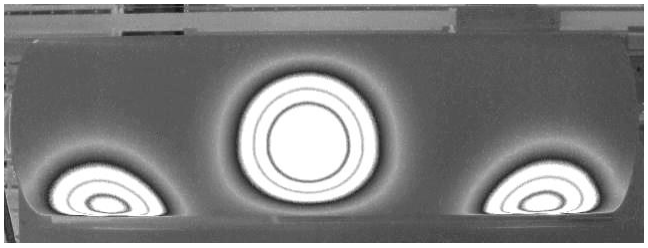

Fig. 3. Typical image seen by the IR camera

Since the camera can see only a part of the heated surface (see Fig. 3), proper algorithms for image concatenation were developed [11]. The processing begins with obtaining a sequence of images (e.g. 8 of them). Images are equally spaced along the perimeter with their acquisition point fixed by the encoder.

In order to retrieve the visible part of the surface, a 3D cylindrical geometry model (5) is used. It is expressed in terms of coordinates on cylinder's surface.

$$Q(u,v) = \left| u\frac{C_L}{T_W} - \frac{C_L}{2}; C_R \sin\left(2\pi\frac{v}{T_H}\right); C_R \cos\left(2\pi\frac{v}{T_H}\right) \right| \tag{5}$$

where: u, v [px] – coordinates of a surface point; C_L, C_R [m] – cylinder's length and radius; T_H, T_W [px] – height and width, of the texture;

By means of reverse mapping (inverted perspective projection) given by (6), one can unwrap a texture from each image of the sequence. This can be seen as an opposite to well-known texturing process in 3D modeling or simply as rectification of curved image. It is worth to note, that only visible part can be unwrapped, as shown in Fig. 4 by hatched area.

$$T(u,v) = \mathrm{Proj}_{M_{cam}} Q(u,v) \tag{6}$$

where: M_{cam} – camera parameters.

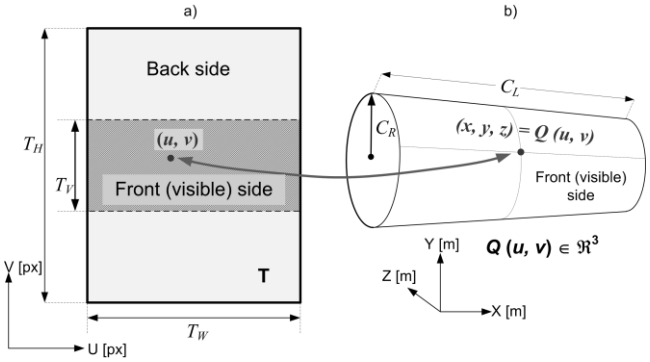

Fig. 4. A reverse mapping from 3D object (visible on an image) to a texture

Camera parameters M_{cam} are selected manually by user or automatically by an algorithm [10]. They allow to mount the camera freely with respect to the object. Such flexibility can be convenient in industrial applications.

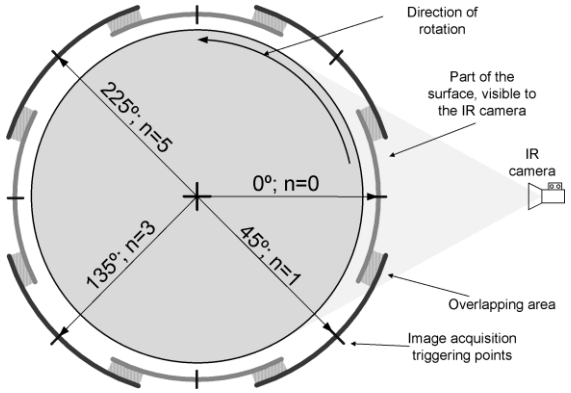

Fig. 5. A sequence of eight images, taken at equally spaced points with overlapping areas visible

Unwrapped set of textures (from a given sequence) have to be concatenated into full temperature map, as show in Fig. 5.

In case of areas, where images are not overlapping, one can simply copy the content into the output temperature image. However in other case, two source of image distortion have to be taken into account. First one is the decreasing resolution caused by curved part of the surface, located near image top and bottom edge. This can be simply overcome by ignoring most distorted areas. Second one is caused by directional emissivity ε [16, 30] and other misuses of infrared sensors [3, 17, 18, 22, 26, 29]. If surface has low values of ε, temperature measurements have to be corrected on basis of angle between surface normal vector and camera optical vector. The resulting part of the output image can be then calculated by means of fuzzy theory [11]. To illustrate the results of such unwrapping-concatenation procedure, an experiment with setup Fig. 6 was conducted. The roller was wound with a resistive wire, connected to an external power supply.

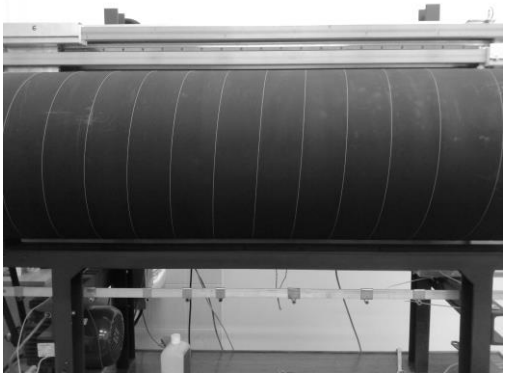

Fig. 6. Experimental setup

A sequence of images was acquired, rectified and concatenated. Obtained result is shown in Fig. 7.

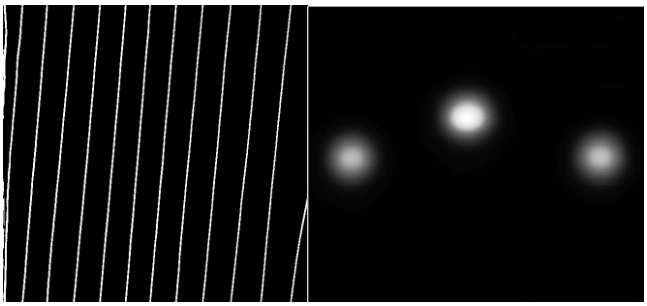

Fig. 7 a) Rectified and concatenated temperature map of heated wire (left); b) temperature map of typical experiment (from sequence with Fig. 3)

Fig. 7 shows a temperature map from a real experiment involving inductive heaters instead of resistive wire. A sample image of the source sequence was previously shown in Fig. 3.

1.3. Image decomposition

In order to proceed with further analysis of visual connectedness, temperature maps have to be transformed into domain of components (2). To obtain a set of components *K*, denoted by **K**, one has to find its cardinality and values of (1). This process is a non-linear optimization (7) where the difference between input image and components' superposition is taken into account.

$$\min_{\mathbf{K}} \sum_{\mathbf{p}} \left(I(\mathbf{p}) - \sum_{n=1}^{|\mathbf{K}|} \Gamma_n(\mathbf{p}) \right)^2 \tag{7}$$

where: I – input image; **K** – sought set of components.

The initial values of **K** are to be found by means of an iterative algorithm, inspired by Mountain Method [2, 14, 20, 32]. During each iteration, the algorithm searches the input image for a point with highest temperature Θ. When found, a new component is generated and stored into **K** with the r value of (1) set to r_{start}. The input image is then destroyed by removing new component from the input image by means of algebraic subtract. The value of r_{start} corresponds to the physical size of the inductive heater and has to be chosen manually. It's value is constant regardless processed temperature map.

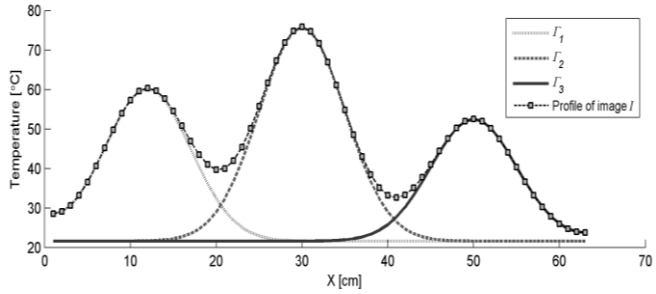

Fig. 8. A visualization of a sample set **K** *consisting of three components $K_{1..3}$ calculated by means of their representations $\Gamma_{1..3}$ (2) with eq. (7)*

The number of components can be limited by their count or difference/distance between original input image and its approximation (4). Although the optimization (7) does not change the number of components, it helps to obtain better approximation (4) by adjusting the r parameter of each component K.

The obtained set **K** is called a *representation of an input image in terms of temperature components.* A proper example was shown in fig. 8, where image I is represented by its profile (arbitrary chosen row or column). Three obtained components are the representation – they are approximation of input profile in terms of eq. (4).

Overall process can be compared to a well-known vectorization of raster images. More details on decomposition can be found in [11].

2. Visual connectedness of two components

The proposed *visual connectedness* evaluation is based on similarity measure [24]. Its goal is to assign a unit degree to a pair of components in similar way that a human expert states "*these two areas of higher temperature are visually connected*". The difference between typical similarity measure and the proposed one is the nature of underlying object. To assess similarity one takes two physically separable objects or states and measures a difference between them. In contrast, the proposed visual connectedness is applicable to objects that can superpose, which is justified by the heat transfer physics intrinsic to component definition given.

Proposed method combines three separate evaluations by means of fuzzy inference, shown in Fig. 9.

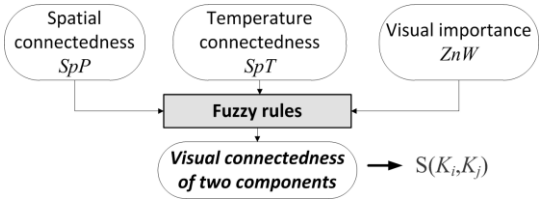

Fig. 9. Fuzzy based visual connectedness evaluation

To obtain full information of set **K** in terms of visual connectedness, one has to calculate its value for each pair of components (K_i, K_j). Such result can be arranged in matrix, alike similarity matrix. A visualization of a sample matrix is shown in Fig. 10.

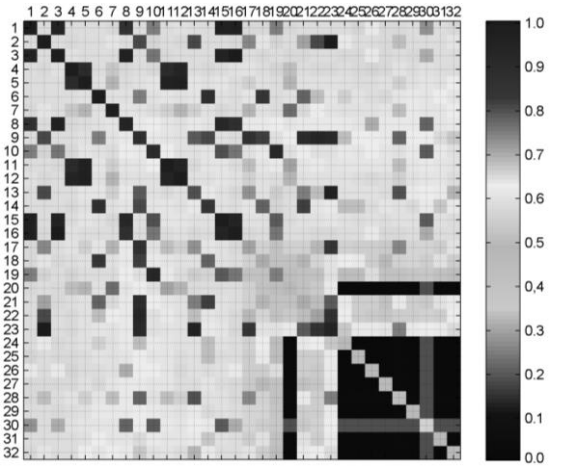

Fig. 10. An example of connectedness matrix. Numbers on both axes denote an index of a component K

It is important to note that both *temperature* and *spatial connectedness* are binary relations of each pair of components (K_i, K_j), resulting in fuzzy variables: *SpP*, *SpT* however *visual importance* is unary with outcome denoted as *ZnW*.

2.1. Visual importance

The assessment of visual importance allows to promote components that are well visible (high Θ) since barely visible ones are canceled out. It is done by calculating membership value of component n to a fuzzy set SMALL (8). Set BIG is given intrinsically.

$$\mu_{small}(\Theta_n) = \frac{1}{1+e^{-a(\Theta_n + c_{SV}\Theta_{max})}}; \quad a = \frac{1}{r_{SV}\Theta_{max}} \ln\left(\frac{1-m_{SV}}{m_{SV}}\right) \tag{8}$$

where: Θ_{max} [°C] – max temperature in whole set **K**; c_{SV} [%] – point of max ambiguity between terms *small* and *big*; r_{SV} [%] – size of ambiguity domain; m_{SV} [-] – value of membership taken by (4) in extremes of ambiguity range, as shown in Fig.11a.

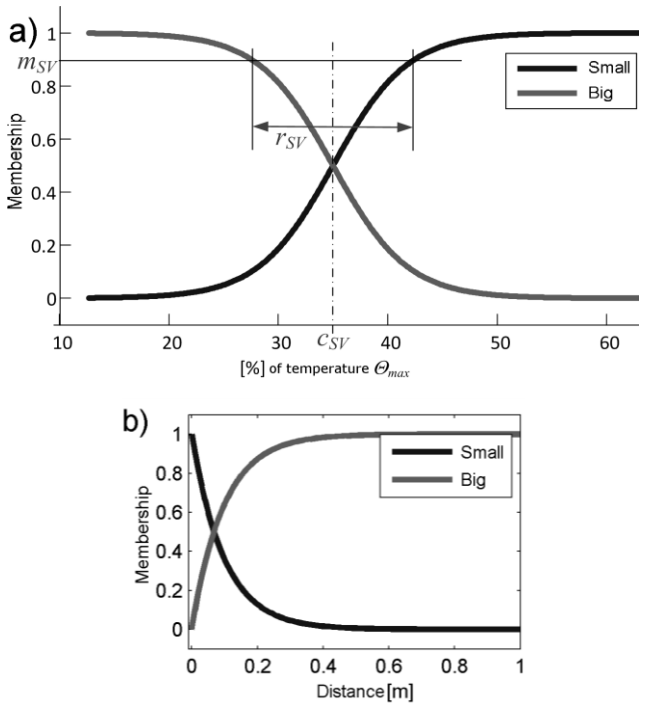

Fig. 11. Membership functions for: a) visual importance; b) spatial connectedness

$$ZnW(K_n)=\begin{cases} s:\mu_{small}(\Theta_n) \\ b:1-\mu_{small}(\Theta_n) \end{cases} \tag{9}$$

Final memberships of fuzzy variable *ZnW* are given by (9). Since *ZnW* is the only unary relation in the proposed evaluation method, its value has to be calculated for both components in pair (K_i, K_j) resulting in two fuzzy variables: ZnW_1 and ZnW_2.

2.2. Spatial connectedness

Spatial connectedness of a pair tells to what degree relations "K_i *is near* K_j" and "K_i *is far form* K_j" hold. It is based on three Euclidean distances (10) from which the lowest is selected (11). This procedure allows to take into account cylindrical surface of the cylinder – when two components are located near top and bottom edge of the image space, they are actually near each other in cylindrical surface space.

$$\begin{aligned} d_0(K_i,K_j)&=\sqrt{(x_i-x_j)^2+(y_i-y_j)^2} \\ d_+(K_i,K_j)&=\sqrt{(x_i-x_j)^2+(y_i-y_j+2\pi C_R)^2} \\ d_-(K_i,K_j)&=\sqrt{(x_i-x_j)^2+(y_i-y_j-2\pi C_R)^2} \end{aligned} \tag{10}$$

$$d(K_i,K_j)=\min\{d_0,d_+,d_-\} \tag{11}$$

The authors have chosen exponential function (12) for the μ_{big} membership, as its values are closest to the human perception [1, 19, 25]. The selected membership function is shown in Fig. 11b.

$$\mu_{big}(d)=e^{-c_1 d} \tag{12}$$

where: c_1[1/m] – slope.

Final assessment is given by a fuzzy variable (13)

$$SpP(K_i,K_j)=\begin{cases} s:\mu_{big}\left(d(K_i,K_j)\right) \\ b:1-\mu_{big}\left(d(K_i,K_j)\right) \end{cases} \tag{13}$$

2.3. Temperature connectedness

The *temperature connectedness* is based on temperature analysis along shortest path between two assessed components, Fig. 12. The shortest path is based on the same principle as the distance (11). For each pixel along such path, a temperature is calculated by means of (4). Obtained values construct a set **Θ**.

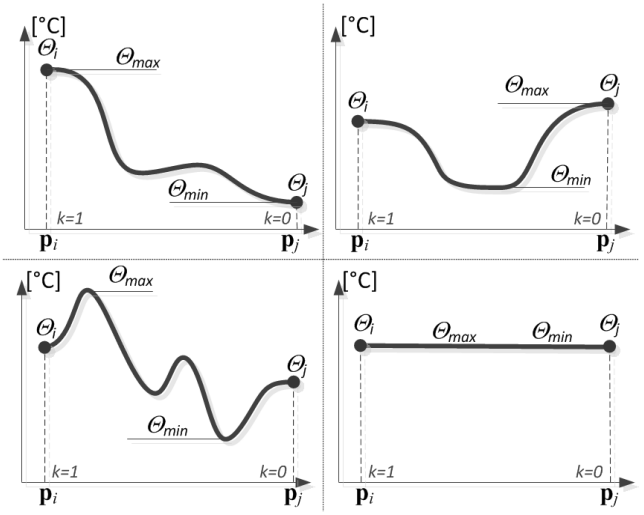

Fig. 12. Temperature plot along shortest path between two (i and j) components; $\mathbf{p}_i$ and $\mathbf{p}_j$ *denotes coordinates of components,* $\mathbf{p}_i=(x_i,y_i)$ *and* $\mathbf{p}_i=(x_j,y_j)$

Conducted experiments show, that this method can be based on temperature ratio of extremes along the path. This assessment is given by (14). Both extremes (Θ_{min} and Θ_{max}) are calculated from superposition of (2) functions over whole set **K**.

$$\mu_{high}(K_i,K_j)=\frac{\Theta_{min}}{\Theta_{max}}=\frac{\min\boldsymbol{\Theta}}{\max\boldsymbol{\Theta}} \tag{14}$$

Final assessment is given by (15).

$$SpT(K_i,K_j)=\begin{cases} h:\mu_{high}(K_i,K_j) \\ l:1-\mu_{high}(K_i,K_j) \end{cases} \tag{15}$$

2.4. Fuzzy inference

In order to obtain a numerical degree of *visual connectedness*, the following set of 16 rules has to be applied to (9), (13) and (15). It is a complete, non-contradictory and non-redundant [21] set of rules – any possible combination of input values has its reflection in corresponding rule. They were formulated by an expert and provide the core of the *visual connectedness* definition.

Unlike parameters (e.g. c_{SV}) previously introduced, the proposed rule base stays constant independently of those parameters. Moreover, not shape of inductive heaters nor dimensions of the roller would affect the rules. This is caused by the fact that rules are separated from the input data by the physical meaning of the fuzzy variables involved.

The output of the rule block used is denoted as fuzzy variable ***S*** and described by three values: **h**igh, **m**edium, **l**ow.

If *SpP* is *b* & *SpT* is *h* & ZnW_1 is *b* & ZnW_2 is *b* then ***S*** is **h**
If *SpP* is *b* & *SpT* is *h* & ZnW_1 is *b* & ZnW_2 is *s* then ***S*** is **m**
If *SpP* is *b* & *SpT* is *h* & ZnW_1 is *s* & ZnW_2 is *b* then ***S*** is **m**
If *SpP* is *b* & *SpT* is *h* & ZnW_1 is *s* & ZnW_2 is *s* then ***S*** is **l**
If *SpP* is *b* & *SpT* is *l* & ZnW_1 is *b* & ZnW_2 is *b* then ***S*** is **l**
If *SpP* is *b* & *SpT* is *l* & ZnW_1 is *b* & ZnW_2 is *s* then ***S*** is **l**
If *SpP* is *b* & *SpT* is *l* & ZnW_1 is *s* & ZnW_2 is *b* then ***S*** is **l**
If *SpP* is *b* & *SpT* is *l* & ZnW_1 is *s* & ZnW_2 is *s* then ***S*** is **l**
If *SpP* is *s* & *SpT* is *h* & ZnW_1 is *b* & ZnW_2 is *b* then ***S*** is **h**
If *SpP* is *s* & *SpT* is *h* & ZnW_1 is *b* & ZnW_2 is *s* then ***S*** is **l**
If *SpP* is *s* & *SpT* is *h* & ZnW_1 is *s* & ZnW_2 is *b* then ***S*** is **l**
If *SpP* is *s* & *SpT* is *h* & ZnW_1 is *s* & ZnW_2 is *s* then ***S*** is **l**
If *SpP* is *s* & *SpT* is *l* & ZnW_1 is *b* & ZnW_2 is *b* then ***S*** is **l**

If *SpP* is *s* & *SpT* is *l* & ZnW_1 is *b* & ZnW_2 is *s* then ***S*** is **l**

If *SpP* is *s* & *SpT* is *l* & ZnW_1 is *s* & ZnW_2 is *b* then ***S*** is **l**

If *SpP* is *s* & *SpT* is *l* & ZnW_1 is *s* & ZnW_2 is *s* then ***S*** is **l**

In every rule of the given set, a consequence uses one of three fuzzy values (h, m, l) assigned to the fuzzy output variable ***S***. Those values are represented by singletons with values respectively 1, 0.5, 0. The inferring model used is TSK (Takagi-Sugeno-Kang) [27, 28], hence final value is calculated with (16).

$$S(K_i, K_j) = \sum_{n=1}^{16} p_n k_n \tag{16}$$

where: p_n [-] – *n*-th rule activation degree, k_n [-] – value of corresponding conclusion.

As for logical conjunction operator, a classical function *min* or *prod* can be used.

3. Conclusion

The proposed method allows to calculate the *visual connectedness* of a pair of components that represent temperature distribution on a cylindrical surface. Extending this calculus through to every pair in **K** leads to a connectedness matrix – a form of similarity matrix.

The values obtained by means of (16) can be further processed via standard approach, e.g. graph-based clusterization methods in order to arrive at image described by components (primitives) and objects (disjoint sets of one or more components).

Constant values used in presented method: c_{SV}, r_{SV}, m_{SV}, c_1, r_{start} have to be chosen manually according to process expert's intuition and knowledge. Assuring proper values of those parameters affects the performance of overall assessment.

In further work, the development of infrared image segmentation algorithm based on human perception of a cylindrical surface, introduced by the described visual connectedness, is planned. It will allow to obtain surface description as a set of consistent spatial and temperature areas. It may for e.g. be a source of information for control decisions. The starting point for such algorithm is taking into account the physical side of the phenomena occurring in the thermal system, in particular the shape of the impulse response generated on the surface of the cylinder. Such approach allows for a significant decrease in information granularity in component-represented image compared to the conventional "pixel" images. Simultaneously it is possible to obtain segmentation results similar to the perception of such images by human.

References

[1] Chater N., Vitanyi P.: The generalized universal law of generalization. Journal of Mathematical Psychology 47/2003, 346-369.
[2] Chiu S.: Fuzzy Model Identification based on cluster estimation. Journal of Intelligent Fuzzy Systems 2/1994, 267-278.
[3] Domke K.: Termowizyjne badanie opraw oświetleniowych. Zeszyty Naukowe Politechniki Łódzkiej - Elektryka Nr 125, 1169/2013, 25-35.
[4] Fogiel M.: Heat Transfer Problem Solver. Research and Eduation Association, 1998.
[5] Frączyk A., Kucharski J., Urbanek P.: Komputerowy system stabilizacji mocy grzejnej w układzie nagrzewania indukcyjnego obracającego się walca. Zeszyty Naukowe Politechniki Świętokrzyskiej 15/2010, Konferencja Modelowanie i Sterowanie Procesów Elektrotermicznych, Kielce 2010, 39-46.
[6] Frączyk A., Urbanek P., Kucharski J.: Control algorithms of induction heating of the rotating steel cylinder with use of moving inductors. Przegląd Elektrotechniczny 86, 2/2010, 42-46.
[7] Frączyk A., Urbanek P., Kucharski J.: Correction algorithms in computerized power control system for induction heating. Automatyka 14/3/1/2010, 423-427.
[8] Gaver N.: Thermography in the Paper Mill - Detecting Moisture Irregularities. Konferencja InfraMation 2000, Infrared Training Center ITC, 2000.
[9] Holman J. P.: Heat transfer. McGraw-Hill, 1986.
[10] Jaworski T., Kucharski J.: An algorithm for finding visual markers in an infrared camera images based on Fuzzy Spatial Relations. Przegląd Elektrotechniczny 89, 2B/2013, 276-279.
[11] Jaworski T., Kucharski J.: An algorithm for reconstruction of temperature distribution on rotating cylinder surface from a thermal camera video stream. Przegląd Elektrotechniczny 89, 2A/2013, 91-94.
[12] Kącki E.: Termokinetyka. Wydawnictwa Naukowo-Techniczne WNT, 1966.
[13] Kucharski J., Urbanek P., Frączyk A., Jaworski T.: Computer-based measurement and control system for induction heating of rotating steel cylinder. Advances in Informatics and Control Engineering, 2013, 133-174.
[14] Lee J., Son S., Kwon S.: Advanced mountain clustering method. Konferencja IFSA World Congress and 20th NAFIPS International Conference, 1/2001, 275-280.
[15] Meyer L., Jayaram S., Cherney E.: Thermal characteristics of filled silicone rubber under laser heating. Electrical Insulation and Dielectric Phenomena, 2003, 383-386.
[16] Michalski L., Eckersdorf K., Kucharski J.: Termometria: Przyrządy i metody. Wydawnictwo Politechniki Łódzkiej, 1998.
[17] Minkina W.A.: Podstawy pomiarów termowizyjnych: Cześć III - Problemy metrologiczne, interpretacja wyników. Pomiary Automatyka Kontrola 11/2001, 5-8.
[18] Minkina W.A.: Podstawy pomiarów termowizyjnych: Cześć IV - Pomiar temperatury ciał półprzezroczystych i poprzez te ciała. Pomiary Automatyka Kontrola 4/2002, 5-8.
[19] Nosofsky R.: Attention, similarity, and the identification-categorization relationship. Journal of Experimental Psychology: General 115/1/1986, 39-57.
[20] Pal N., Chakraborty D.: Mountain and subtractive clustering method: Improvements and generalizations. International Journal of Intelligent Systems 15, 4/2000, 329-341.
[21] Piegat A.: Modelowanie i sterowanie rozmyte. Akademicka Oficyna Wydawnicza EXIT, 2003.
[22] Radomiak H., Musiał D., Zajemska M.: The use of contactless methods in the study of metallic stock surface temperature. Przegląd Elektrotechniczny 89, 12/2013, 95-99.
[23] Rosenthal D.: The theory of moving sources of heat and its application to metal treatments. Transactions of the American Society of Mechanical Engineeriners 68/1946, 849–866.
[24] Santini S., Jain R.: Similarity measures. IEEE Transactions on Pattern Analysis and Machine Intelligence 21/9/1999, 871–883.
[25] Shepard R. N.: Towards a universal law of generalization for psychological science. Science 237/1987, 1317-1323.
[26] Styła S.: Examination of an electromagnetic mill structure by means of infrared radiation. Przegląd Elektrotechniczny 90, 3/2014, 179-182.
[27] Sugeno M., Kang G.: Structure identification of fuzzy model. Fuzzy Sets and Systems 28/1/1988, 15-33.
[28] Takagi T., Sugeno M.: Fuzzy identification of systems and its applications to modeling and control. Systems, Man and Cybernetics, IEEE Transactions on SMC-15, 1/1985, 116-132.
[29] Wesołowski M., Niedbała R., Kucharski D.: Thermovision techniques precision of temperature measurement. Przegląd Elektrotechniczny 85, 12/2009, 208-211.
[30] Więcek B., De Mey G.: Termowizja w podczerwienie. Podstawy i zastosowania. Wydawnictwo PAK, Warszawa 2011.
[31] Wiśniewski S., Wiśniewski T.: Wymiana ciepła, Wydawnictwa Naukowo-Techniczne WNT, 2000.
[32] Yager R., Filev D.: Approximate Clustering Via the Mountain Method. Systems, Man and Cybernetics, IEEE Transactions 24/8/1994, 1279-1284.

M.Sc. Tomasz Jaworski
e-mail: tjaworski@iis.p.lodz.pl

Tomasz Jaworski is a Ph.D. student at Lodz University of Technology (TUL), Institute of Applied Computer Science. His scientific interest covers artificial intelligence, image processing and electronics. He is author and co-author of nearly 30 papers and chapters.

Prof. Jacek Kucharski
e-mail: jkuchars@iis.p.lodz.pl

Prof. J. Kucharski obtained his Ph.D. degree in 1993 and D.Sc. degree in 2004. Currently he holds a position of associate professor at Lodz University of Technology (TUL). Since 2012 he serves as a deputy head of Institute of Applied Computer Science at TUL. His scientific interest covers application of computational intelligence in various areas, especially in industrial processes. Prof. J.Kucharski is an author or co-author of more than 130 scientific papers, books and chapters.

otrzymano/received: 08.10.2014 *przyjęto do druku/accepted: 04.12.2014*